Impact Factor:					
	ISRA (India) = 6.317	SIS (USA) = 0.912	ICV (Poland) = 6.630
	ISI (Dubai, UAE) = 1.582	РИНЦ (Russia) = 3.939	PIF (India) = 1.940
	GIF (Australia) = 0.564	ESJI (KZ) = 8.771	IBI (India) = 4.260
	JIF = 1.500	SJIF (Morocco) = 7.184	OAJI (USA) = 0.350

SOI: 1.1/TAS DOI: 10.15863/TAS
International Scientific Journal
Theoretical & Applied Science
p-ISSN: 2308-4944 (print) **e-ISSN:** 2409-0085 (online)
Year: 2022 **Issue:** 07 **Volume:** 111
Published: 18.07.2022 **http://T-Science.org**

Issue Article

Denis Chemezov
Vladimir Industrial College
M.Sc.Eng., Corresponding Member of International Academy of Theoretical and Applied Sciences, Lecturer, Russian Federation
https://orcid.org/0000-0002-2747-552X
vic-science@yandex.ru

Aleksey Kuzin
Vladimir Industrial College
Student, Russian Federation

Andrey Karasyov
Vladimir Industrial College
Student, Russian Federation

Anton Ilin
Vladimir Industrial College
Student, Russian Federation

Vladislav Zaychukhin
Vladimir Industrial College
Student, Russian Federation

REFERENCE DATA OF PRESSURE DISTRIBUTION ON THE SURFACES OF AIRFOILS HAVING THE NAMES BEGINNING WITH THE LETTER L

Abstract: *The results of the computer calculation of air flow around the airfoils having the names beginning with the letter L are presented in the article. The contours of pressure distribution on the surfaces of the airfoils at the angles of attack of 0, 15 and -15 degrees in conditions of the subsonic airplane flight speed were obtained.*

Key words: *the airfoil, the angle of attack, pressure, the surface.*
Language: *English*
Citation: Chemezov, D., et al. (2022). Reference data of pressure distribution on the surfaces of airfoils having the names beginning with the letter L. *ISJ Theoretical & Applied Science, 07 (111),* 101-118.
Soi: http://s-o-i.org/1.1/TAS-07-111-12 ***Doi***: crossref https://dx.doi.org/10.15863/TAS.2022.07.111.12
Scopus ASCC: *1507.*

Introduction

Creating reference materials that determine the most accurate pressure distribution on the airfoils surfaces is an actual task of the airplane aerodynamics.

Materials and methods

The study of air flow around the airfoils was carried out in a two-dimensional formulation by means of the computer calculation in the *Comsol Multiphysics* program. The airfoils in the cross section were taken as objects of research [1-27]. In this work, the airfoils having the names beginning with the letter *L* were adopted. Air flow around the airfoils was carried out at the angles of attack (α) of 0, 15 and -15 degrees. Flight speed of the airplane in each case was subsonic. The airplane flight in the atmosphere was carried out under normal weather conditions. The geometric characteristics of the studied airfoils are

presented in the Table 1. The geometric shapes of the airfoils in the cross section are presented in the Table 2.

Table 1. The geometric characteristics of the airfoils.

Airfoil name	Max. thickness	Max. camber	Leading edge radius	Trailing edge thickness
LA203A	15.73% at 34.3% of the chord	5.48% at 46.0% of the chord	3.0242%	0.0%
LDS-2	11.97% at 34.9% of the chord	2.16% at 45.0% of the chord	1.0915%	0.0%
LI-CA-CO	7.3% at 25.0% of the chord	7.3% at 40.0% of the chord	0.8042%	0.9%
LINDNER1	5.92% at 20.0% of the chord	6.16% at 40.0% of the chord	1.4329%	0.25%
LINDNER2	6.65% at 20.0% of the chord	6.88% at 50.0% of the chord	0.7091%	0.4%
Lippisch 301 G	9.8% at 25.0% of the chord	10.05% at 30.0% of the chord	1.4012%	0.3%
LISSAMAN 7769	10.98% at 30.0% of the chord	4.43% at 30.0% of the chord	1.4998%	0.0%
LNV109A	12.99% at 23.5% of the chord	5.97% at 31.5% of the chord	3.4968%	0.0%
LNV203A	15.73% at 34.3% of the chord	5.48% at 46.0% of the chord	3.0235%	0.0%
LOCKHEED C-141 BL0	12.99% at 40.2% of the chord	1.09% at 64.5% of the chord	1.6191%	0.1096%
LOCKHEED C-141 BL113,6	12.64% at 40.2% of the chord	1.12% at 64.5% of the chord	1.5382%	0.1234%
LOCKHEED C-141 BL426,57	10.99% at 40.2% of the chord	1.32% at 50.0% of the chord	1.1663%	0.1854%
LOCKHEED C-141 BL610,61	10.77% at 40.2% of the chord	1.54% at 50.0% of the chord	1.5044%	0.2188%
LOCKHEED C-141 BL761,11	10.51% at 40.2% of the chord	1.8% at 50.0% of the chord	1.6226%	0.2546%
LOCKHEED C-141 BL958,89	10.0% at 40.2% of the chord	2.32% at 45.1% of the chord	2.1456%	0.3249%
LOCKHEED C-5A BL0	13.12% at 40.0% of the chord	0.73% at 85.0% of the chord	1.0842%	0.2578%
LOCKHEED C-5A BL1256	10.78% at 40.0% of the chord	1.43% at 30.0% of the chord	1.5955%	0.2013%
LOCKHEED C-5A BL488.2	11.55% at 40.0% of the chord	1.22% at 70.0% of the chord	1.0667%	0.22%
LOCKHEED C-5A BL576	11.1% at 40.0% of the chord	1.4% at 65.0% of the chord	1.0637%	0.219%
LOCKHEED C-5A BL758.6	11.05% at 40.0% of the chord	1.35% at 60.0% of the chord	1.1819%	0.222%
LOCKHEED L-188 ROOT	13.99% at 41.3% of the chord	2.0% at 51.7% of the chord	1.9032%	0.28%
LOCKHEED L-188 TIP	11.99% at 41.3% of the chord	2.66% at 51.7% of the chord	1.4116%	0.24%
Lockheed-Georgia C-5A	13.12% at 40.0% of the chord	0.73% at 85.0% of the chord	1.083%	0.258%
LOCKHEED-GEORGIA SUPERCRITICAL	10.0% at 32.0% of the chord	1.46% at 16.0% of the chord	0.9893%	0.3%
Lockheed-Georgia/NASA/Blackwell	10.0% at 32.0% of the chord	1.46% at 16.0% of the chord	0.9893%	0.3%
lrn1007	7.27% at 39.8% of the chord	5.9% at 44.6% of the chord	0.216%	0.0%

Note:
LA203A (Douglas/Liebeck LA203A high lift airfoil);
Lippisch 301 G (A. Lippisch (Germany));
LISSAMAN 7769 (Lissaman 7769 human powered aircraft airfoil);
LNV109A (Douglas/Liebeck LNV109A high lift airfoil);
LOCKHEED L-188 ROOT (Lockheed L-188/P-3 root airfoil NACA 0014 -1.10 40/1.051 Cli=.3 a=.8);
LOCKHEED L-188 TIP (Lockheed L-188/P-3 tip airfoil NACA 0012 -1.10 40/1.051 Cli=.4 a=.8);
Lockheed-Georgia C-5A (Transonic wing airfoil);
LOCKHEED-GEORGIA SUPERCRITICAL (Lockheed-Georgia/NASA/Blackwell rotorcraft airfoil);
Lockheed-Georgia/NASA/Blackwell (Rotorcraft airfoil);
lrn1007 (RN(1)-1007 low Reynolds number airfoil).

Table 2. The geometric shapes of the airfoils in the cross section.

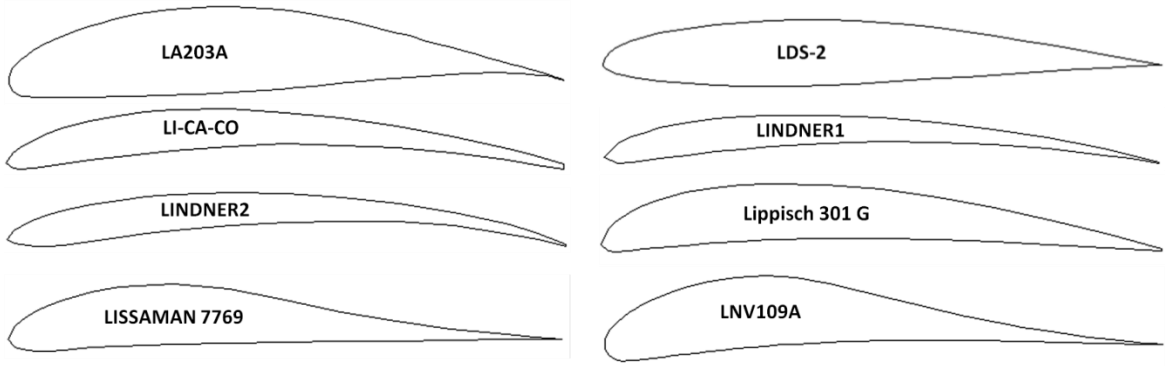

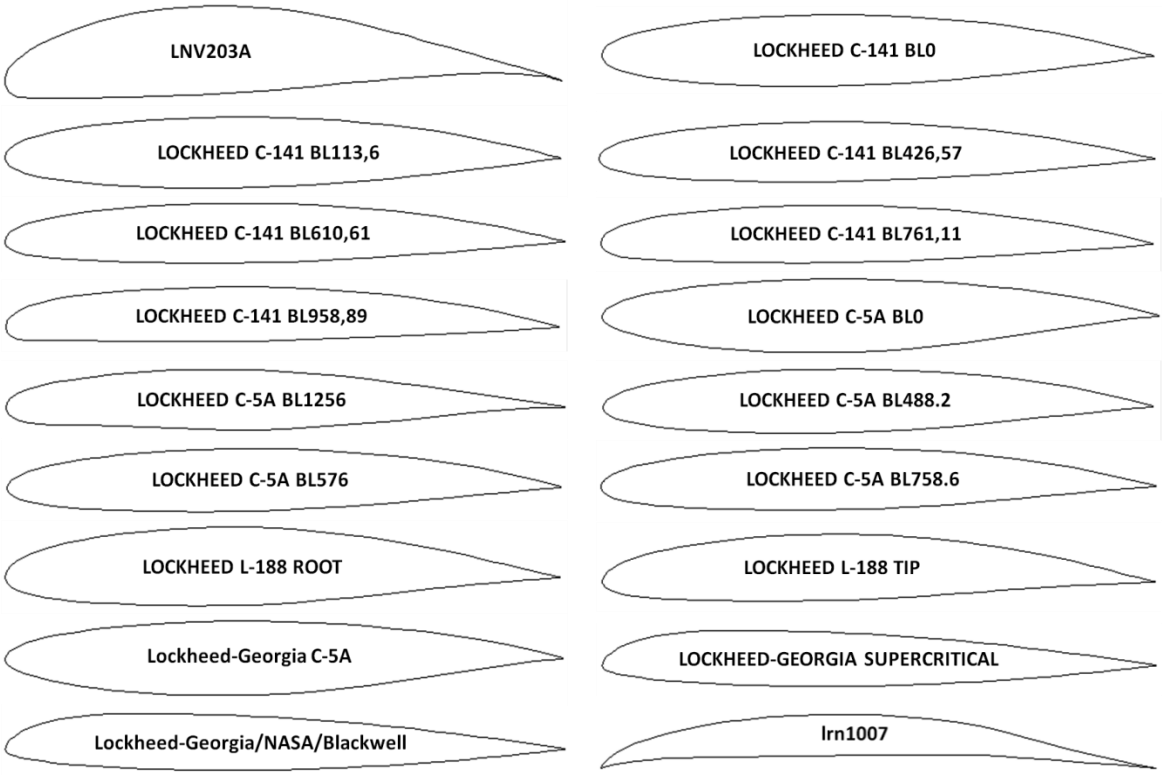

Results and discussion

The calculated pressure contours on the surfaces of the airfoils at the different angles of attack are presented in the Figs. 1-26. The calculated values on the scale can be represented as the basic values when comparing the pressure drop under conditions of changing the angle of attack of the airfoils.

26 airfoils of the LOCKHEED, LNV, LINDNER, etc. series were considered. All airfoils had camber of the various value. Thus, all airfoils were asymmetrical.

The drag was determined from the calculated pressure contours on the leading edge of the airfoils. The lower the calculated pressure on the edge, the better the aerodynamic characteristics of the airplane wing. Positive pressure occurs on the leading edge during horizontal flight. The change in the pressure values varies within 0.17 kPa. The slight change in pressure does not give an idea of the more favorable airfoil configuration. Therefore, the lift to drag ratio of the airplane wing can be determined from the pressure distribution area. However, the minimum pressure value (6.42 kPa), and hence the drag coefficient, was determined for the LOCKHEED C-141 BL958,89 airfoil, and the maximum pressure value (6.59 kPa) was determined for the LINDNER2 airfoil.

With an increase in the contact area of the airfoils with air flows, positive pressure increases and negative pressure arises on the leading edge and on the upper and lower surfaces. This happens under conditions of the airplane maneuvers. The maneuvers are climb and descent of the airplane. In this case, the maximum value of negative pressure was determined on the leading edge of the airfoil. The maximum and minimum values were identified after analyzing the calculated pressures values on the leading edge. Pressure of -68.1 kPa acts on the LINDNER2 airfoil at the positive angle of attack, and pressure of -67.6 kPa acts on the LDS-2 airfoil at the negative angle of attack, which is the highest value of pressures of all calculated values. The minimum pressures values of -27.3 kPa and -6.04 kPa were determined for the LNV109A and lrn1007 airfoils at the positive and negative angles of attack, respectively. Thus, the LNV109A and lrn1007 airfoils have the best aerodynamic properties.

Let us consider these airfoils in detail. The values of the maximum camber of both airfoils are the same and are about 6% relative to the chord length. However, under conditions of the airplane climb, the drag decreases with the large radius of the leading edge of the airfoil. This phenomenon is provided by the airfoil with the small radius of the leading edge during the airplane descent.

The LINDNER2 and LDS-2 airfoils (where high pressure occurs) have the opposite geometric parameters compared to the geometric parameters of the LNV109A and lrn1007 airfoils.

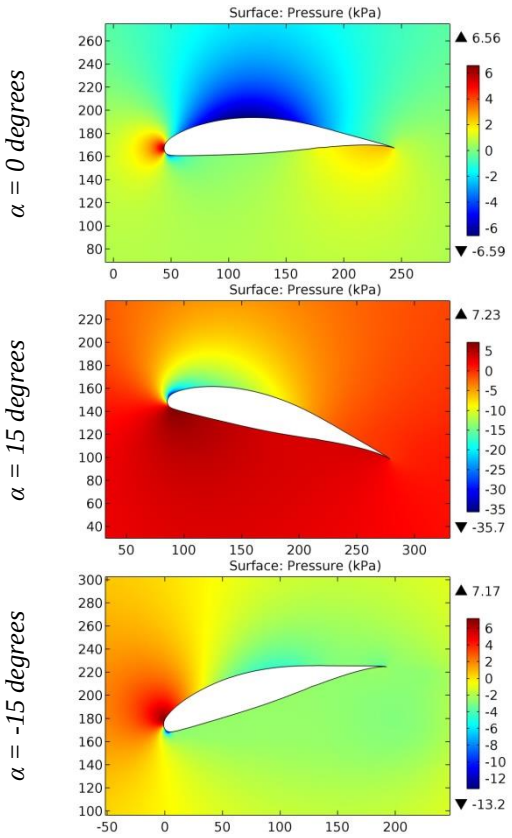

Figure 1. The pressure contours on the surfaces of the LA203A airfoil.

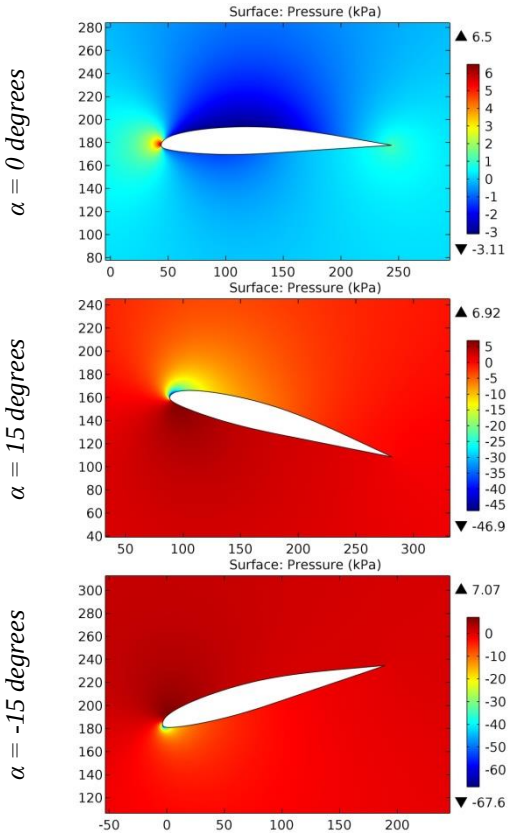

Figure 2. The pressure contours on the surfaces of the LDS-2 airfoil.

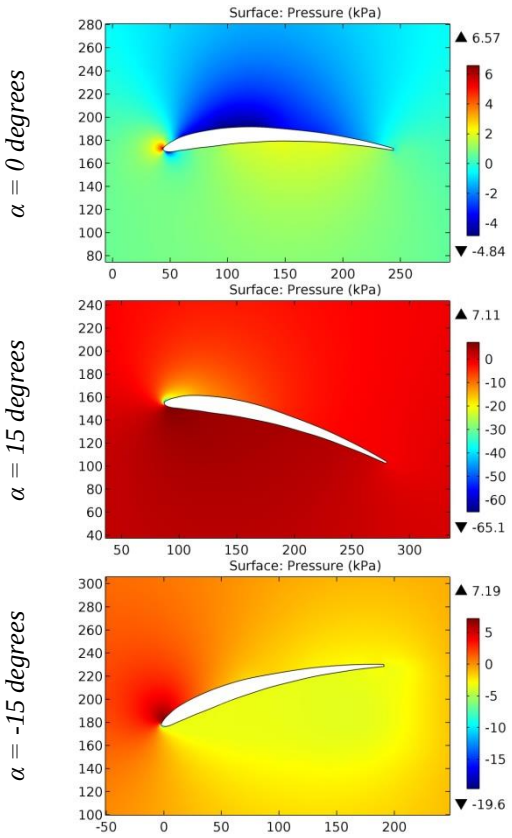

Figure 3. The pressure contours on the surfaces of the LI-CA-CO airfoil.

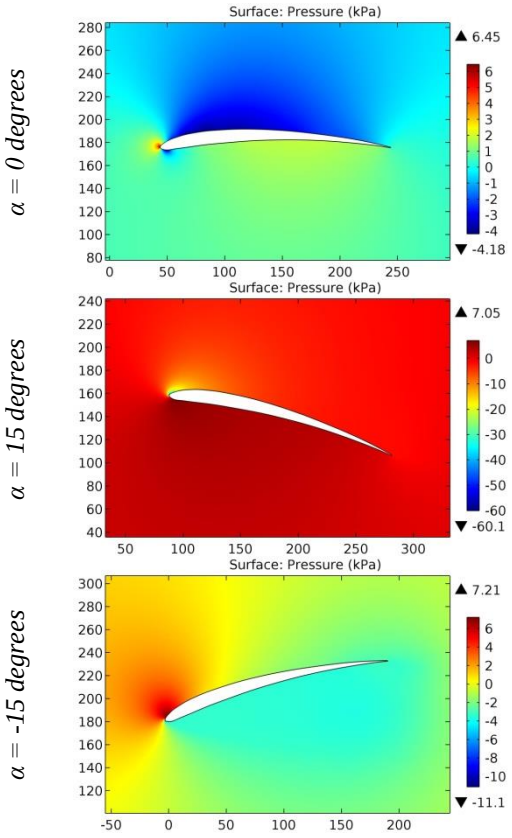

Figure 4. The pressure contours on the surfaces of the LINDNER1 airfoil.

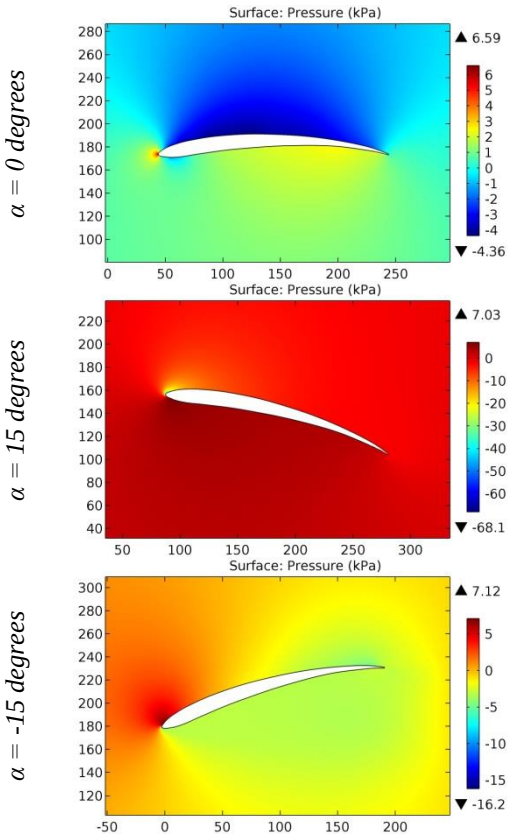

Figure 5. The pressure contours on the surfaces of the LINDNER2 airfoil.

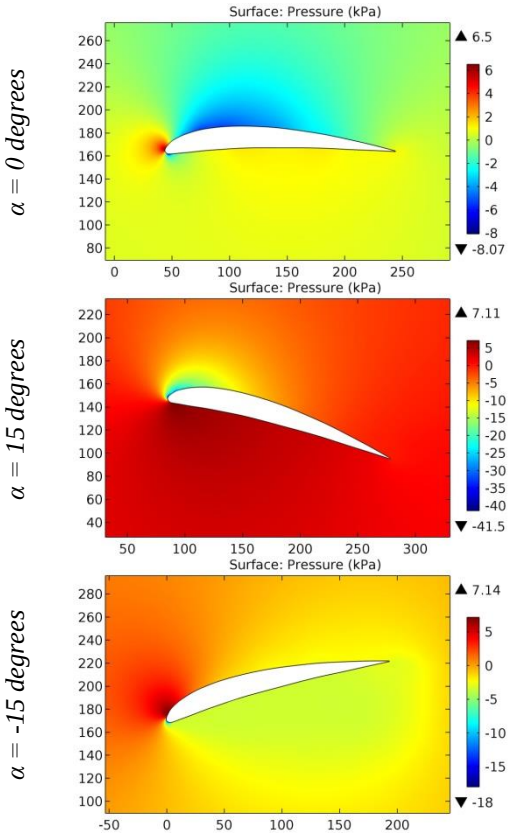

Figure 6. The pressure contours on the surfaces of the Lippisch 301 G airfoil.

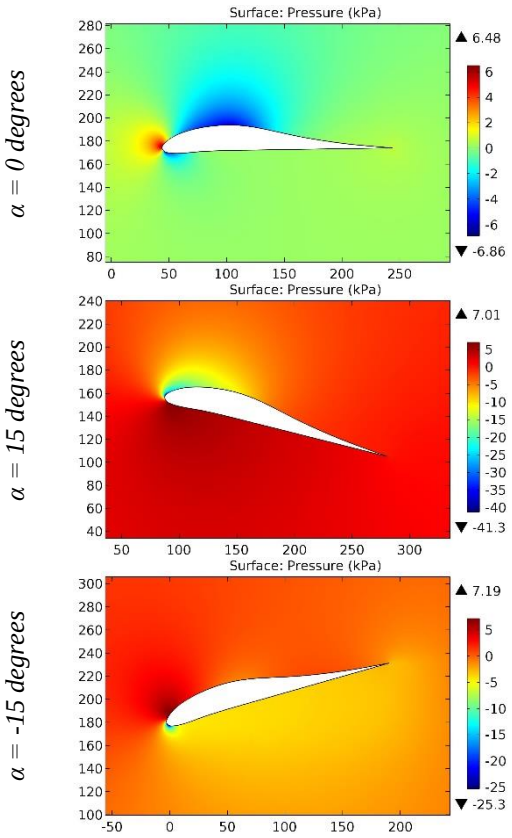

Figure 7. The pressure contours on the surfaces of the LISSAMAN 7769 airfoil.

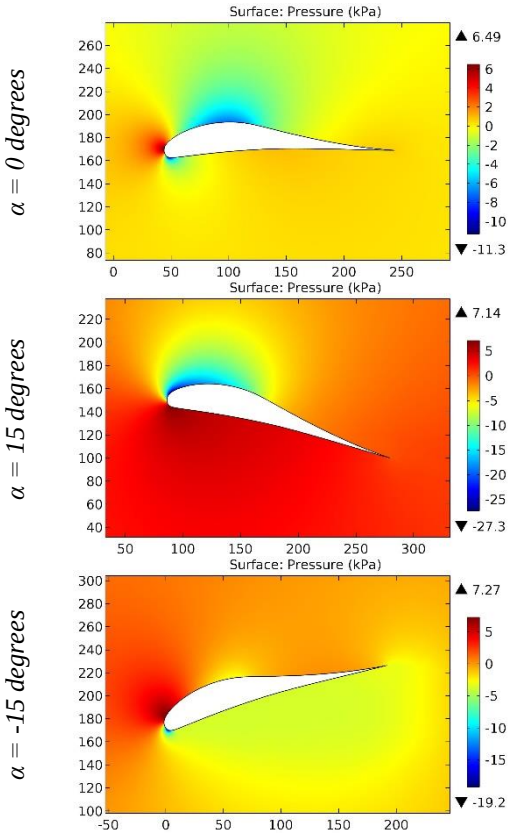

Figure 8. The pressure contours on the surfaces of the LNV109A airfoil.

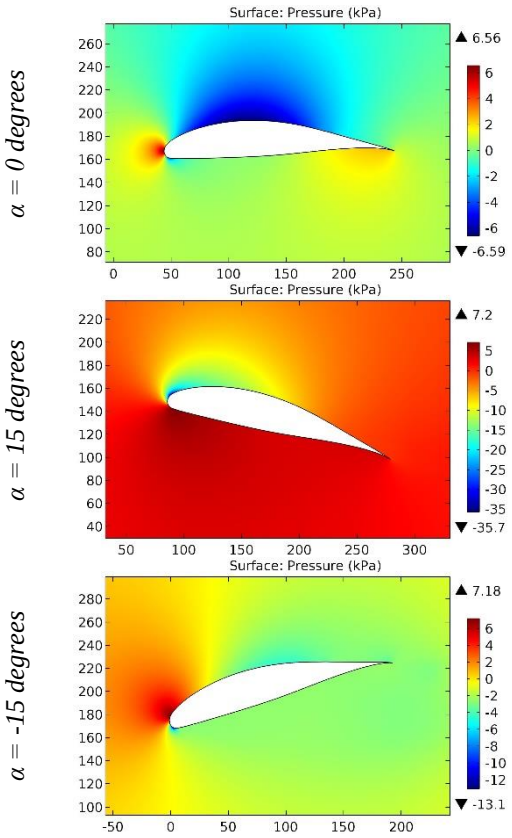

Figure 9. The pressure contours on the surfaces of the LNV203A airfoil.

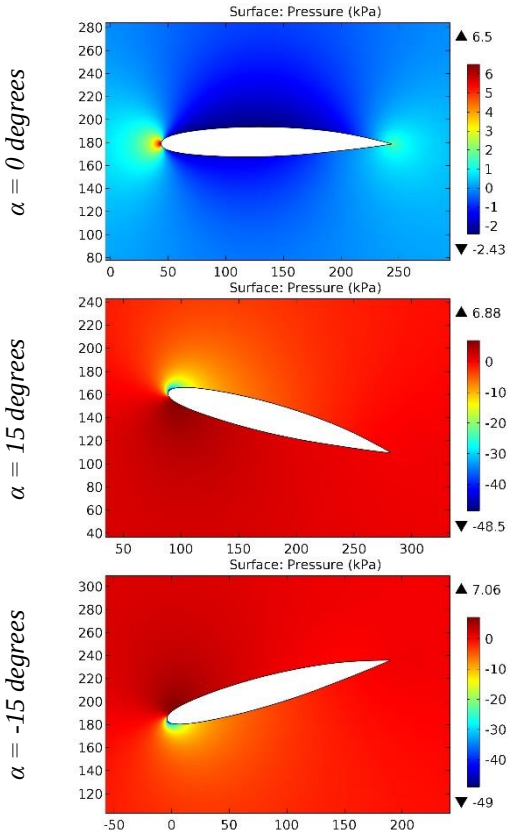

Figure 10. The pressure contours on the surfaces of the LOCKHEED C-141 BL0 airfoil.

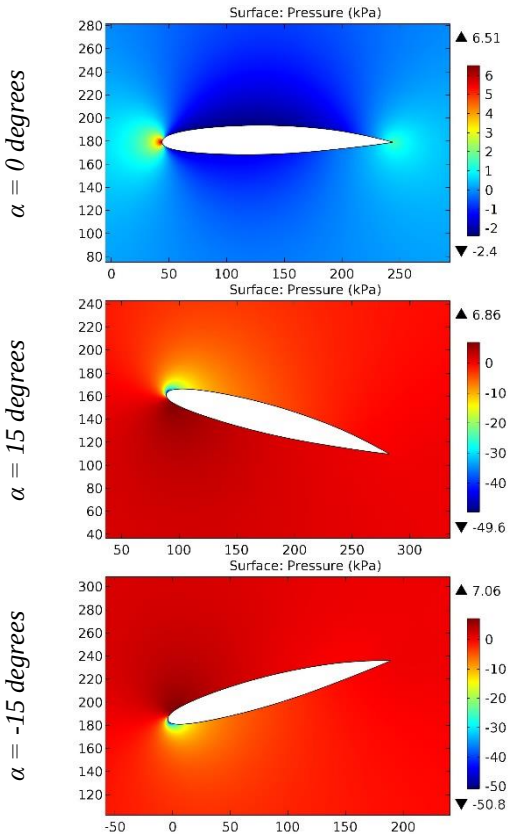

Figure 11. The pressure contours on the surfaces of the LOCKHEED C-141 BL113,6 airfoil.

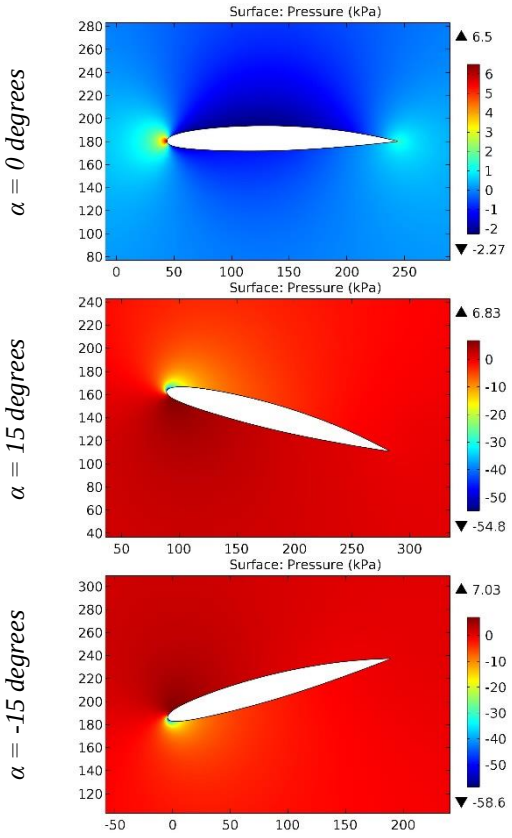

Figure 12. The pressure contours on the surfaces of the LOCKHEED C-141 BL426,57 airfoil.

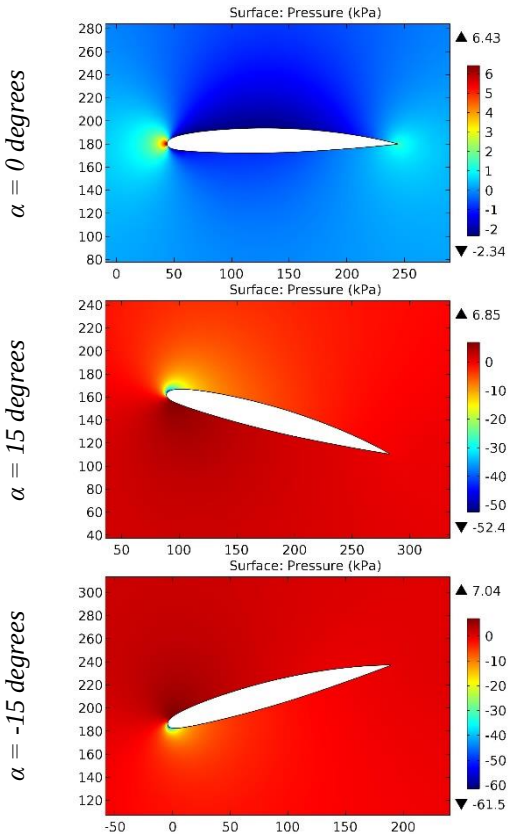

Figure 13. The pressure contours on the surfaces of the LOCKHEED C-141 BL610,61 airfoil.

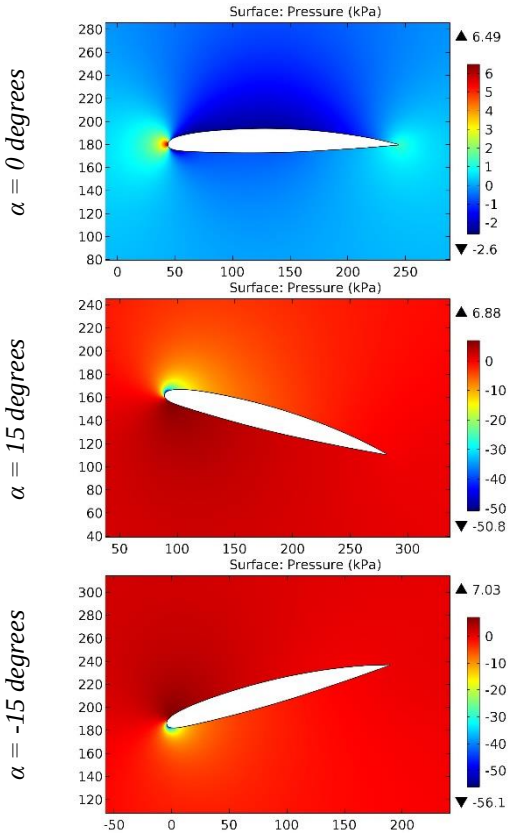

Figure 14. The pressure contours on the surfaces of the LOCKHEED C-141 BL761,11 airfoil.

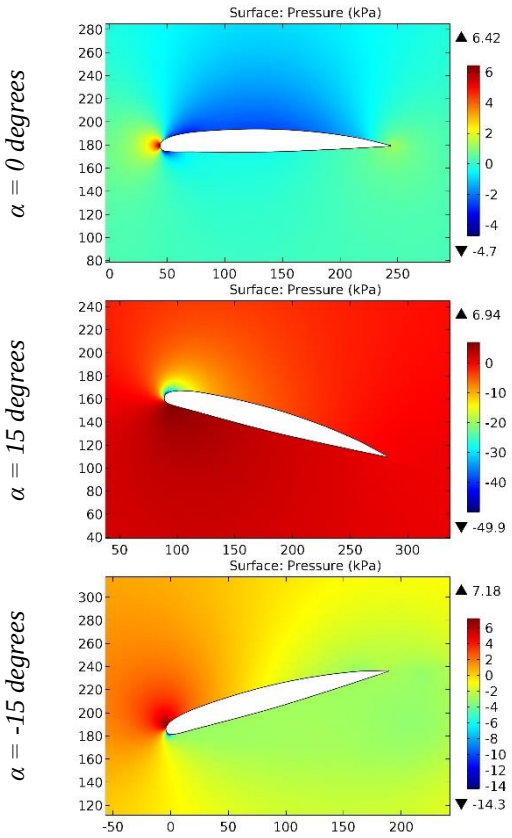

Figure 15. The pressure contours on the surfaces of the LOCKHEED C-141 BL958,89 airfoil.

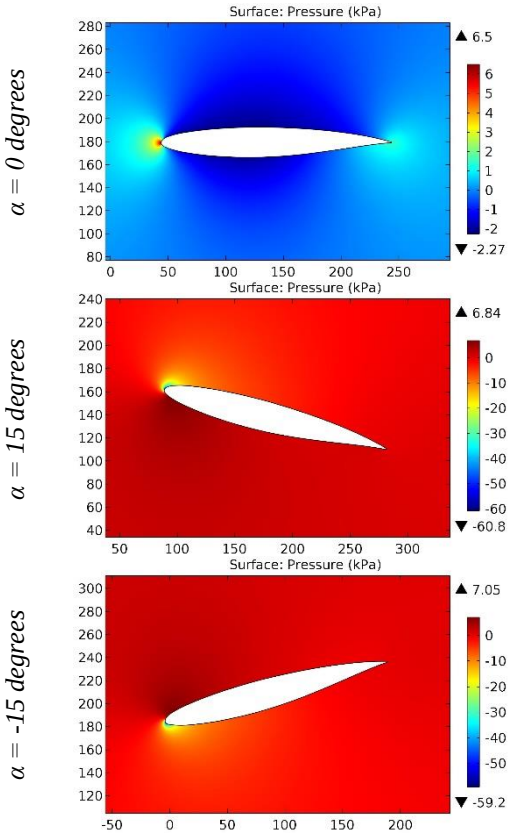

Figure 16. The pressure contours on the surfaces of the LOCKHEED C-5A BL0 airfoil.

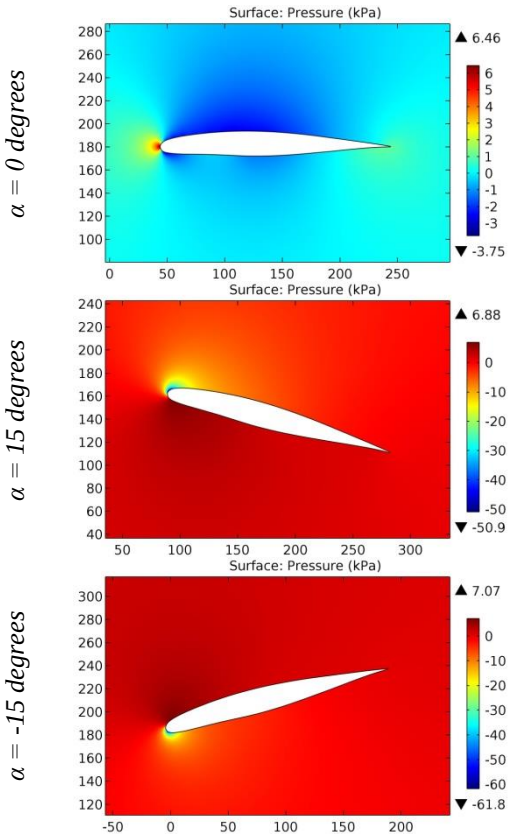

Figure 17. The pressure contours on the surfaces of the LOCKHEED C-5A BL1256 airfoil.

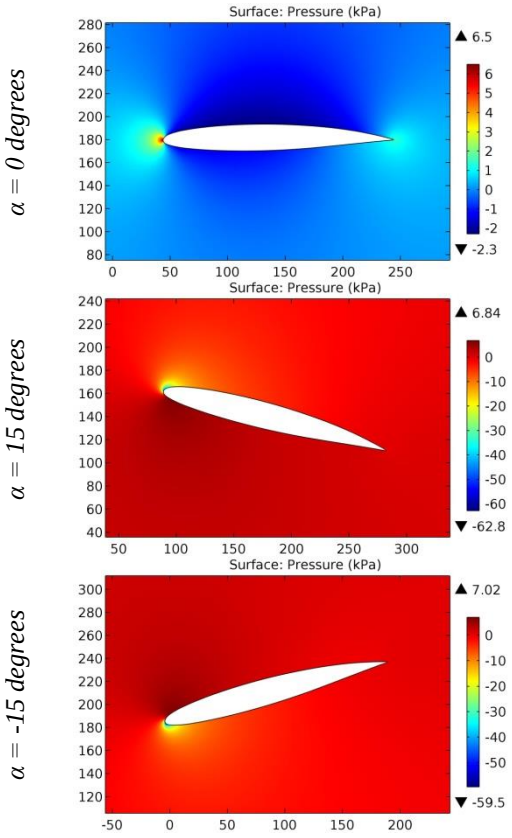

Figure 18. The pressure contours on the surfaces of the LOCKHEED C-5A BL488.2 airfoil.

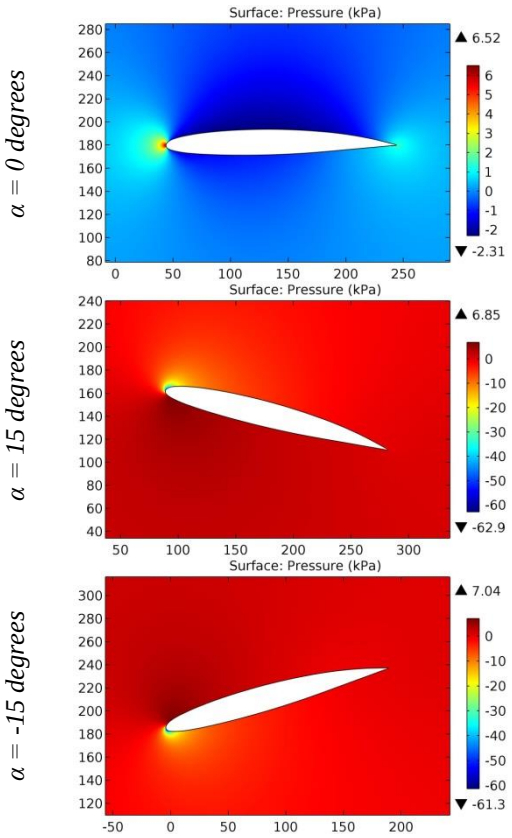

Figure 19. The pressure contours on the surfaces of the LOCKHEED C-5A BL576 airfoil.

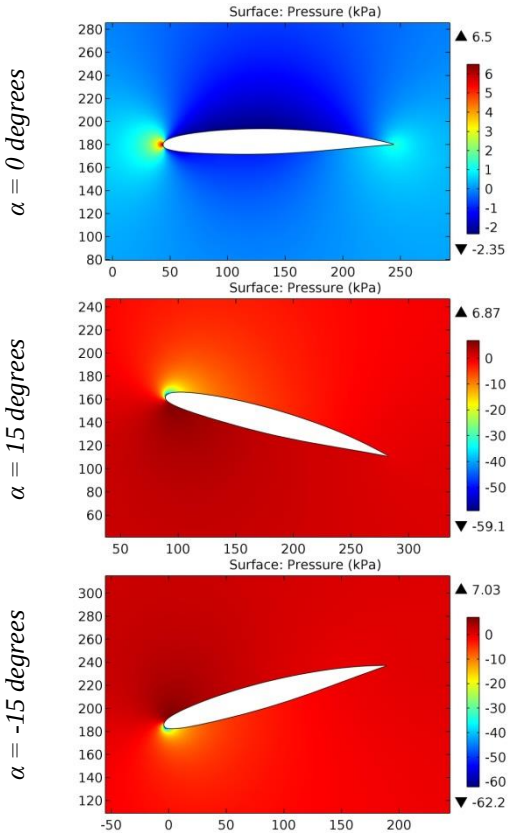

Figure 20. The pressure contours on the surfaces of the LOCKHEED C-5A BL758.6 airfoil.

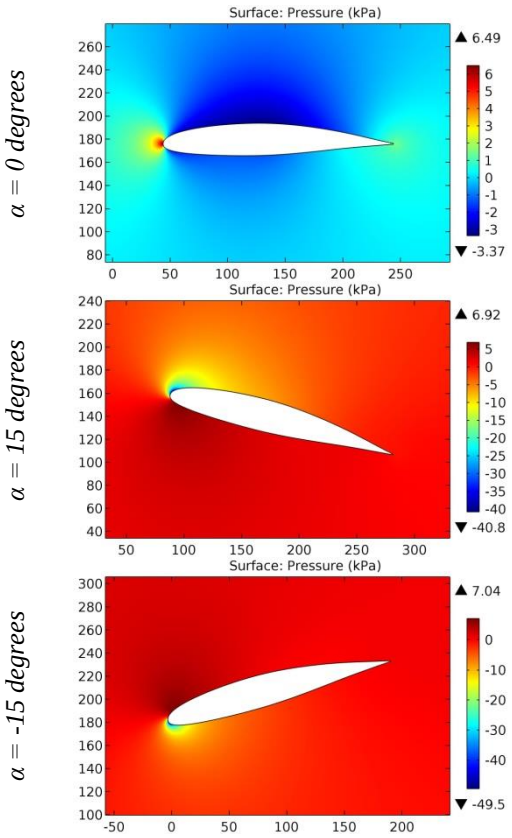

Figure 21. The pressure contours on the surfaces of the LOCKHEED L-188 ROOT airfoil.

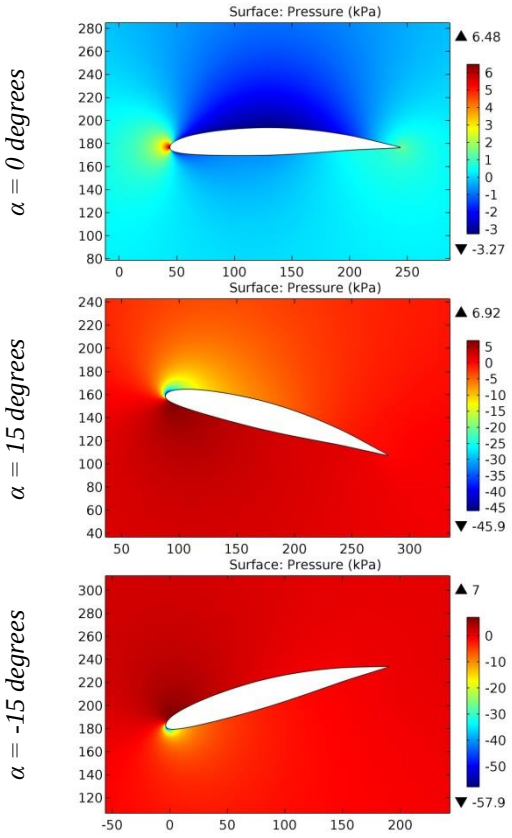

Figure 22. The pressure contours on the surfaces of the LOCKHEED L-188 TIP airfoil.

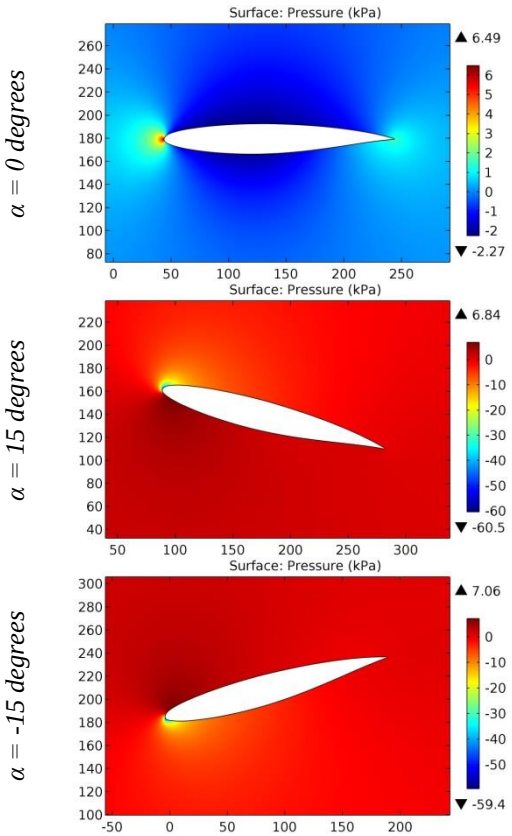

Figure 23. The pressure contours on the surfaces of the Lockheed-Georgia C-5A airfoil.

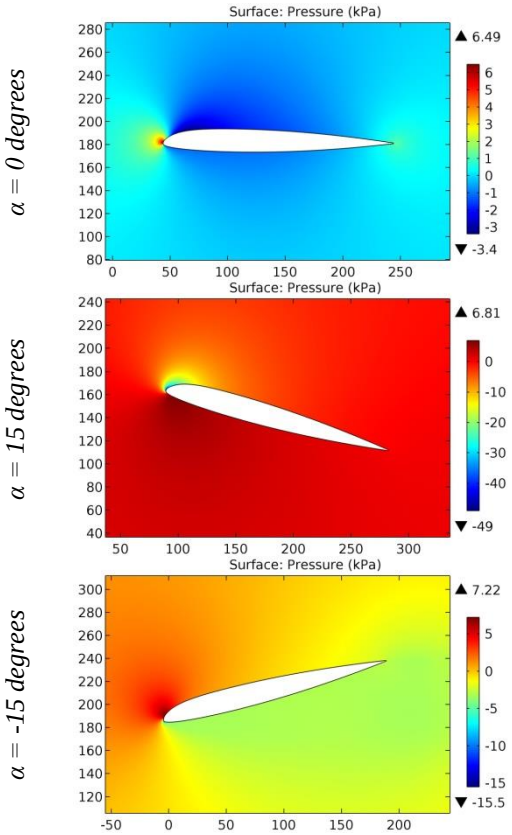

Figure 24. The pressure contours on the surfaces of the LOCKHEED-GEORGIA SUPERCRITICAL airfoil.

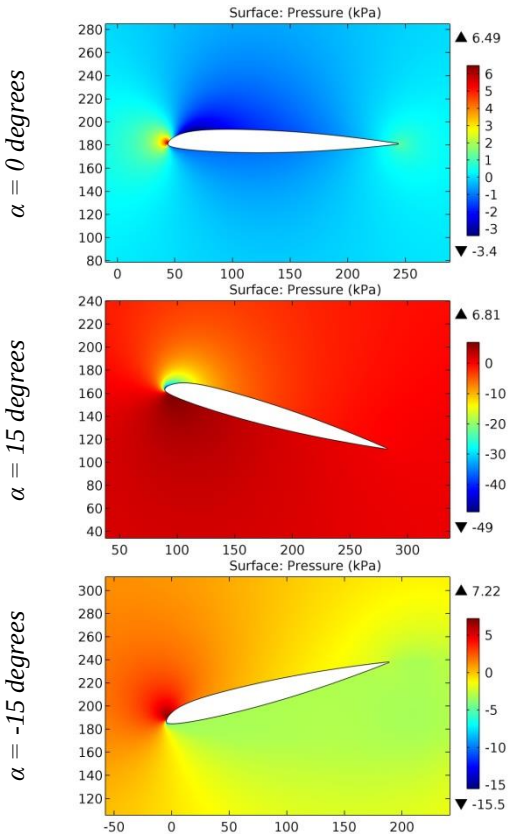

Figure 25. The pressure contours on the surfaces of the Lockheed-Georgia/NASA/Blackwell airfoil.

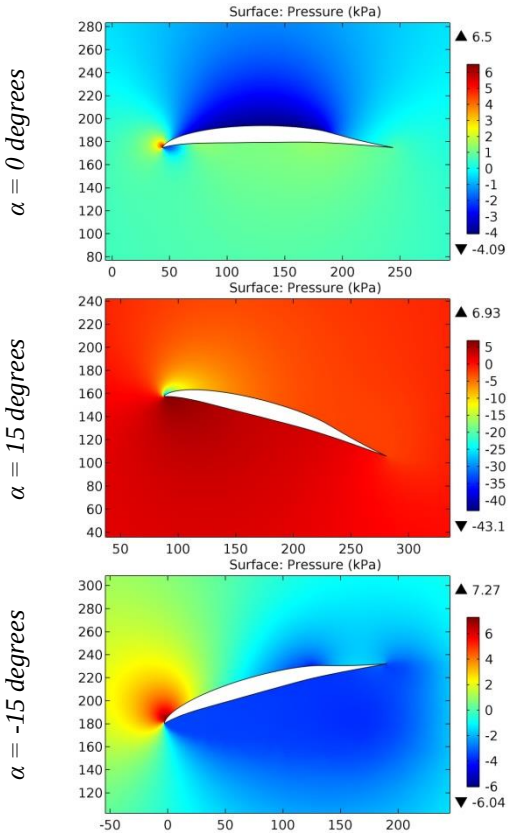

Figure 26. The pressure contours on the surfaces of the lrn1007 airfoil.

Conclusion

The calculation results make it possible to compare the aerodynamic characteristics of the airplanes wings of the various configurations. Since the large drag on the leading edge reduces the aerodynamic characteristics of the airplane wing, the purpose of this study was to determine and analyze the airfoils that are subjected to minimal pressures during horizontal flight and maneuvers of the airplane. According to this indicator, some airfoils were identified (LINDNER2, LDS-2, LNV109A and lrn1007). After comparing these airfoils, it was concluded that the maximum camber of the airfoil during the airplane maneuvers should vary in the range from 3% to 6% relative to the chord length, and the radius of the leading edge during climb and descent of the airplane should be at least 3.5% and 0.2%, respectively. These geometric parameters of the airfoils improve the aerodynamic characteristics of the airplane.

References:

1. Anderson, J. D. (2010). *Fundamentals of Aerodynamics.* McGraw-Hill, Fifth edition.
2. Shevell, R. S. (1989). *Fundamentals of Flight.* Prentice Hall, Second edition.
3. Houghton, E. L., & Carpenter, P. W. (2003). *Aerodynamics for Engineering Students*. Fifth edition, Elsevier.
4. Lan, E. C. T., & Roskam, J. (2003). *Airplane Aerodynamics and Performance.* DAR Corp.
5. Sadraey, M. (2009). *Aircraft Performance Analysis.* VDM Verlag Dr. Müller.
6. Anderson, J. D. (1999). *Aircraft Performance and Design.* McGraw-Hill.
7. Roskam, J. (2007). *Airplane Flight Dynamics and Automatic Flight Control*, Part I. DAR Corp.
8. Etkin, B., & Reid, L. D. (1996). *Dynamics of Flight, Stability and Control.* Third Edition, Wiley.
9. Stevens, B. L., & Lewis, F. L. (2003). *Aircraft Control and Simulation.* Second Edition, Wiley.
10. Chemezov, D., et al. (2021). Pressure distribution on the surfaces of the NACA 0012 airfoil under conditions of changing the angle of attack. *ISJ Theoretical & Applied Science, 09 (101)*, 601-606.
11. Chemezov, D., et al. (2021). Stressed state of surfaces of the NACA 0012 airfoil at high angles of attack. *ISJ Theoretical & Applied Science, 10 (102)*, 601-604.
12. Chemezov, D., et al. (2021). Reference data of pressure distribution on the surfaces of airfoils having the names beginning with the letter A (the first part). *ISJ Theoretical & Applied Science, 10 (102)*, 943-958.
13. Chemezov, D., et al. (2021). Reference data of pressure distribution on the surfaces of airfoils having the names beginning with the letter A (the second part). *ISJ Theoretical & Applied Science, 11 (103)*, 656-675.
14. Chemezov, D., et al. (2021). Reference data of pressure distribution on the surfaces of airfoils having the names beginning with the letter B. *ISJ Theoretical & Applied Science, 11 (103)*, 1001-1076.
15. Chemezov, D., et al. (2021). Reference data of pressure distribution on the surfaces of airfoils having the names beginning with the letter C. *ISJ Theoretical & Applied Science, 12 (104)*, 814-844.
16. Chemezov, D., et al. (2021). Reference data of pressure distribution on the surfaces of airfoils having the names beginning with the letter D. *ISJ Theoretical & Applied Science, 12 (104)*, 1244-1274.
17. Chemezov, D., et al. (2022). Reference data of pressure distribution on the surfaces of airfoils (hydrofoils) having the names beginning with the letter E (the first part). *ISJ Theoretical & Applied Science, 01 (105)*, 501-569.
18. Chemezov, D., et al. (2022). Reference data of pressure distribution on the surfaces of airfoils (hydrofoils) having the names beginning with the letter E (the second part). *ISJ Theoretical & Applied Science, 01 (105)*, 601-671.
19. Chemezov, D., et al. (2022). Reference data of pressure distribution on the surfaces of airfoils having the names beginning with the letter F. *ISJ Theoretical & Applied Science, 02 (106)*, 101-135.
20. Chemezov, D., et al. (2022). Reference data of pressure distribution on the surfaces of airfoils having the names beginning with the letter G (the first part). *ISJ Theoretical & Applied Science, 03 (107)*, 701-784.

21. Chemezov, D., et al. (2022). Reference data of pressure distribution on the surfaces of airfoils having the names beginning with the letter G (the second part). *ISJ Theoretical & Applied Science, 03 (107)*, 901-984.
22. Chemezov, D., et al. (2022). Reference data of pressure distribution on the surfaces of airfoils having the names beginning with the letter G (the third part). *ISJ Theoretical & Applied Science, 04 (108)*, 401-484.
23. Chemezov, D., et al. (2022). Reference data of pressure distribution on the surfaces of airfoils having the names beginning with the letter H (the first part). *ISJ Theoretical & Applied Science, 05 (109)*, 201-258.
24. Chemezov, D., et al. (2022). Reference data of pressure distribution on the surfaces of airfoils having the names beginning with the letter H (the second part). *ISJ Theoretical & Applied Science, 05 (109)*, 529-586.
25. Chemezov, D., et al. (2022). Reference data of pressure distribution on the surfaces of airfoils having the names beginning with the letter I. *ISJ Theoretical & Applied Science, 06 (110)*, 1-7.
26. Chemezov, D., et al. (2022). Reference data of pressure distribution on the surfaces of airfoils having the names beginning with the letter J. *ISJ Theoretical & Applied Science, 06 (110)*, 18-25.
27. Chemezov, D., et al. (2022). Reference data of pressure distribution on the surfaces of airfoils having the names beginning with the letter K. *ISJ Theoretical & Applied Science, 07 (111)*, 1-10.